

A brief review of recent advances on the Mott transition: unconventional transport, spectral weight transfers, and critical behaviour

A. Georges^a, S. Florens^b and T.A. Costi^b

^aLPT - Ecole Normale Supérieure 24, rue Lhomond 75231 Paris Cedex 05

and: CPHT - Ecole Polytechnique, 91128 Palaiseau Cedex; e-mail: antoine.georges@cpht.polytechnique.fr

^bInstitut für Theorie der Kondensierten Materie, Universität Karlsruhe, Postfach 6980, 76128 Karlsruhe; e-mail: florens@tkm.physik.uni-karlsruhe.de (S.Florens), tac@tkm.physik.uni-karlsruhe.de (T. Costi)

Abstract. Strongly correlated metals close to the Mott transition display unusual transport regimes, together with large spectral weight transfers in optics and photoemission. We briefly review the theoretical understanding of these effects, based on the dynamical mean-field theory, and emphasize the key role played by the two energy scales associated with quasiparticle coherence scale and with the Mott gap. Recent experimental results on two-dimensional organic compounds and transition metal oxides are considered in this perspective. The liquid-gas critical behaviour at the Mott critical endpoint is also discussed. Transport calculations using the numerical renormalization group are presented.

Keywords. Mott transition - Organic conductors - Vanadium oxide - Bad metals - Dynamical Mean-Field Theory - Liquid-gas transition.

To appear in: Proceedings of the Vth International Conference on Crystalline Organic Metals, Superconductors and Magnets (ISCOM 2003) to be published in Journal de Physique IV (EDP Sciences).

1. MATERIALS ON THE VERGE OF THE MOTT TRANSITION

The Mott phenomenon - that interactions between electrons can be responsible for the insulating character of a material - plays a key role in the physics of strongly correlated electron materials. Outstanding examples [1] are transition-metal oxides (e.g superconducting cuprates), fullerene compounds, as well as organic conductors. A limited number of these materials are poised right on the verge of this electronic instability. This is the case, for example, of V_2O_3 , $NiS_{2-x}Se_x$ and of quasi two-dimensional organic conductors of the κ -BEDT family. These materials are particularly interesting for the fundamental investigation of the Mott transition, since they offer the possibility of going from one phase to the other by varying some external parameter (e.g chemical composition, temperature, pressure,...). Varying external pressure is definitely a tool of choice since it allows to sweep continuously from the insulating phase to the metallic phase (and back). The phase diagrams of $(V_{1-x}Cr_x)_2O_3$ and of κ -(BEDT-TTF)₂Cu[N(CN)₂]Cl under pressure are displayed in Fig. 1.

There is a great similarity between the high-temperature part of the phase diagrams of these materials, despite very different energy scales. At low-pressure they are *paramagnetic* Mott insulators, which are turned into metals as pressure is increased. Above a critical temperature T_c (of order ~ 450 K for the oxide compound and ~ 40 K for the organic one), this corresponds to a smooth crossover. In contrast, for $T < T_c$ a first-order transition is observed, with a discontinuity of all physical observables (e.g resistivity). The first order transition line ends in a second order critical endpoint at (T_c, P_c) . We observe that in both cases, the critical temperature is a very small fraction of the bare electronic energy scales (for V_2O_3 the half-bandwidth is of order 0.5 – 1 eV, while it is of order 2000 K for the organics).

There are also some common features between the low-temperature part of the phase diagram of these compounds, such as the fact that the paramagnetic Mott insulator orders into an antiferromagnet as tem-

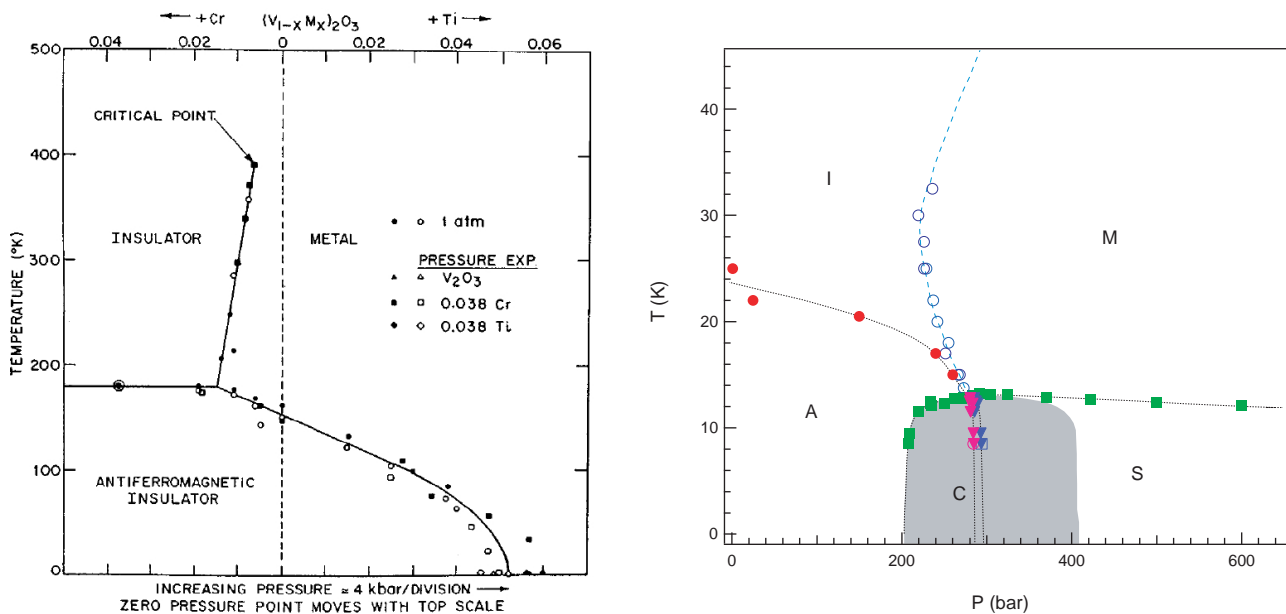


Figure 1: Phase diagram of $(V_{1-x}Cr_x)_2O_3$ (left, after [7]) and of κ -(BEDT-TTF) $_2$ Cu[N(CN) $_2$]Cl (right, after [8]), as a function of Cr-concentration and pressure (left), and of pressure (right).

perature is lowered. However, there are also striking differences: the metallic phase has a superconducting instability for the organics, while this is not the case for V_2O_3 . Also, the magnetic transition is only superficially similar: in the case of V_2O_3 , it is widely believed to be accompanied (or even triggered) by orbital ordering [2] (in contrast to $NiS_{2-x}Se_x$ [3]), and as a result the transition is first-order. In general, there is a higher degree of universality associated with the vicinity of the Mott critical endpoint than in the low-temperature region, in which long-range order takes place in a material-specific manner.

Mott localization into a paramagnetic insulator implies a high spin entropy, which must therefore be quenched in some way as temperature is lowered. An obvious possibility is magnetic ordering, as in these two materials. In fact, a Mott transition between a paramagnetic Mott insulator and a metallic phase is only observed in those compounds where magnetism is sufficiently *frustrated* so that the transition is not preempted by magnetic ordering. This is indeed the case in both compounds discussed here: V_2O_3 has competing ferromagnetic and antiferromagnetic exchange constants, while the two-dimensional layers in the organics have a triangular structure. Another possibility is that the entropy is quenched through a Peierls instability (dimerization), in which case the Mott insulator can remain paramagnetic (this is the case, for example, of VO_2). Whether it is possible to stabilize a paramagnetic Mott insulator down to $T = 0$ without breaking spin or translational symmetries is a fascinating problem, both theoretically and from the materials point of view (for a recent review on resonating valence bond phases in frustrated quantum magnets, see e.g [4]). As discussed by Kanoda at this conference [5], the compound κ -(BEDT-TTF) $_2$ Cu $_2$ (CN) $_3$ may offer a realization of such a spin-liquid state (presumably through a combination of strong frustration and strong charge fluctuations [6]), but this behaviour is certainly more the exception than the rule.

2. DYNAMICAL MEAN-FIELD THEORY AND TWO KEY ENERGY SCALES

Over the last decade, a detailed theory of the strongly correlated metallic state, and of the Mott transition itself has emerged, based on the *dynamical mean-field theory* (DMFT). We refer to [9] for a review and an extensive list of original references. Some key features of this theory are the following [10]:

- In the metallic state, Fermi-liquid theory applies below a low energy scale ε_F^* , which can be interpreted as the coherence-scale for quasiparticles. This low-energy coherence scale is given by

$\varepsilon_F^* \sim ZD$ (with D the half-bandwidth, also equal to the Fermi energy of the non-interacting system at half-filling) where Z is the quasiparticle weight. In the strongly correlated metal close to the transition, $Z \ll 1$, so that ε_F^* is strongly reduced as compared to the bare Fermi energy.

- In addition to low-energy quasiparticles (carrying a fraction Z of the spectral weight), the one-particle spectrum of the strongly correlated metal contains high-energy excitations carrying a spectral weight $1 - Z$. These are associated to the atomic-like transitions corresponding to the addition or removal of one electron on an atomic site, which broaden into Hubbard bands in the solid. As a result, the \mathbf{k} -integrated spectral function $A(\omega) = \sum_{\mathbf{k}} A(\mathbf{k}, \omega)$ (density of states d.o.s) of the strongly correlated metal is predicted [11] to display a three-peak structure, made of a quasiparticle band close to the Fermi energy surrounded by lower and upper Hubbard bands (Fig. 3). The quasiparticle part of the d.o.s has a reduced width of order $ZD \sim \varepsilon_F^*$. The lower and upper Hubbard bands are separated by an energy scale Δ .
- At strong enough coupling (see below), the paramagnetic solution of the DMFT equations is a Mott insulator, with a gap Δ in the one-particle spectrum. This phase is characterized by unscreened local moments, associated with a Curie law for the local susceptibility $\sum_q \chi_q \propto 1/T$, and an extensive entropy (note however that the uniform susceptibility $\chi_{q=0}$ is finite, of order $1/J \sim U/D^2$). As temperature is lowered, these local moments order into an antiferromagnetic phase [12]. The Néel temperature is however strongly dependent on frustration [9, 10] (e.g on the ratio t'/t between the next nearest-neighbour and nearest-neighbour hoppings) and can be made vanishingly small for fully frustrated models.

Within DMFT, a separation of energy scales holds close to the Mott transition. The mean-field solution corresponding to the paramagnetic metal at $T = 0$ disappears at a critical coupling U_{c2} . At this point, the quasiparticle weight vanishes ($Z \propto 1 - U/U_{c2}$) as in Brinkman-Rice theory. On the other hand, a mean-field insulating solution is found for $U > U_{c1}$, with the Mott gap Δ opening up at this critical coupling (Mott-Hubbard transition). As a result, Δ is a finite energy scale for $U = U_{c2}$ and the quasiparticle peak in the d.o.s is well separated from the Hubbard bands in the strongly correlated metal.

These two critical couplings extend at finite temperature into two spinodal lines $U_{c1}(T)$ and $U_{c2}(T)$, which delimit a region of the $(U/D, T/D)$ parameter space in which two mean-field solutions (insulating and metallic) are found (Fig. 2). Hence, within DMFT, a first-order Mott transition occurs at finite temperature even in a purely electronic model. The corresponding critical temperature T_c^{el} is of order $T_c^{el} \sim \Delta E / \Delta S$, with ΔE and $\Delta S \sim \ln(2S + 1)$ the energy and entropy differences between the metal and the insulator. Because the energy difference is small ($\Delta E \sim (U_{c2} - U_{c1})^2 / D$), the critical temperature is much lower than D and U_c (by almost two orders of magnitude).

The existence of well- formed (lower) Hubbard bands in correlated metals was established experimentally more than ten years ago in the pioneering work [13] of Fujimori and coworkers on the photoemission spectra of d^1 transition metal oxides. A clear demonstration of the narrow quasiparticle peak in $A(\omega)$ predicted by DMFT close to the transition came only recently however (see [14] for the metallic phase of V_2O_3 and [15] for $NiS_{2-x}Se_x$). In the case of V_2O_3 , this was made possible by the use of high-energy photons in photoemission spectroscopy, allowing to overcome the surface sensitivity of this technique. This also proved essential in resolving a long-standing controversy on the spectroscopy of $Ca_{1-x}Sr_xVO_3$ [16, 17].

The quasiparticle peak in the d.o.s is characterized by an extreme sensitivity to changes of temperature (inset of Fig. 3). Its height is strongly reduced as T is increased, and the peak disappears altogether as T reaches ε_F^* , leaving a pseudogap at the Fermi energy. Indeed, above ε_F^* , long-lived coherent quasiparticles no longer exist. The corresponding spectral weight is redistributed over a very large range of energies, of order U . These spectral weight transfers and redistributions are a distinctive feature of strongly correlated systems, and have been observed e.g in the optical conductivity of both metallic V_2O_3 [18] and the organics [19]. This is reminiscent of Kondo systems [20], and indeed DMFT establishes a formal and physical connection [11] between a metal close to the Mott transition and the Kondo problem. The local moment

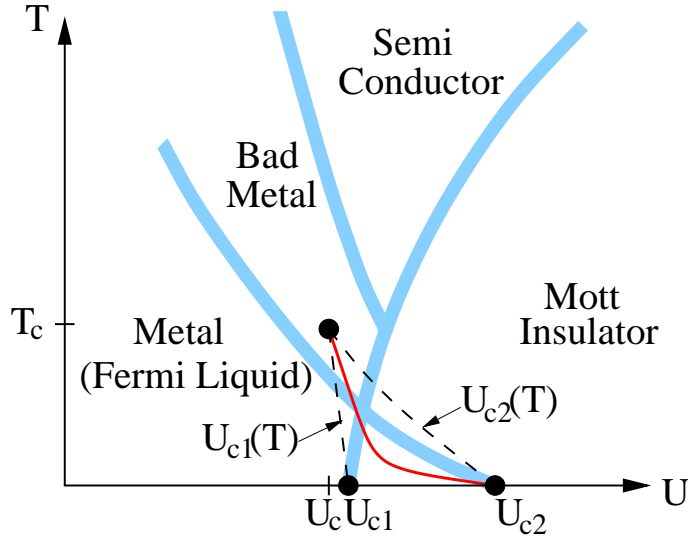


Figure 2: Paramagnetic phases of the Hubbard model within DMFT, displaying schematically the spinodal lines of the Mott insulating and metallic mean-field solutions (dashed), the first-order transition line (plain) and the critical endpoint. The shaded crossover lines separating the different transport regimes discussed in Sec.3 are also shown. The Fermi-liquid to “bad metal” crossover line corresponds to the quasiparticle coherence scale and is a continuation of the spinodal $U_{c2}(T)$ above T_c . The crossover into the insulating state corresponds to the continuation of the U_{c1} spinodal. Magnetic phases are not displayed and depend on the degree of frustration

present at short time-scales is screened through a self-consistent Kondo process involving the low-energy part of the (single- component) electronic fluid itself.

3. TRANSPORT REGIMES AND CROSSOVERS

The disappearance of coherent quasiparticles, and associated spectral changes, results in three distinct transport regimes [18, 21, 22, 23] for a correlated metal close to the Mott transition, within DMFT (Figs. 2 and 3):

- In the *Fermi-liquid regime* $T \ll \varepsilon_F^*$, the resistivity obeys a T^2 law with an enhanced prefactor: $\rho = \rho_M (T/\varepsilon_F^*)^2$. In this expression, ρ_M is the Mott-Ioffe-Regel resistivity $\rho_M \propto \hbar a/e^2$ corresponding to a mean-free path of the order of a single lattice spacing in a Drude picture.
- For $T \sim \varepsilon_F^*$, an “*incoherent*” (or “*bad*”) *metal* regime is entered. The quasiparticle lifetime shortens dramatically, and the quasiparticle peak is strongly suppressed (but still present). In this regime, the resistivity is metallic-like (i.e increases with T) but reaches values considerably larger than the Mott “limit” ρ_M . A Drude description is no longer applicable in this regime.
- Finally, for $\varepsilon_F^* \ll T \ll \Delta$, quasiparticles are gone altogether and the d.o.s displays a pseudogap associated with the scale Δ and filled with thermal excitations. This yields a *semi-conducting* regime of transport, with the resistivity decreasing upon heating. Hence, the temperature dependence of the resistivity displays a maximum (Fig. 3). This maximum is observed experimentally in both Cr-doped V_2O_3 and the organics.

Within DMFT, the conductivity can be simply obtained from a calculation of the one-particle self-energy since vertex corrections are absent. However, a precise determination of both the real and imaginary part of the real-frequency self-energy is required. This is a challenge for most “impurity solvers”. In practice, early calculations[21, 18, 22] used the iterated perturbation theory (IPT) approximation[11]. The

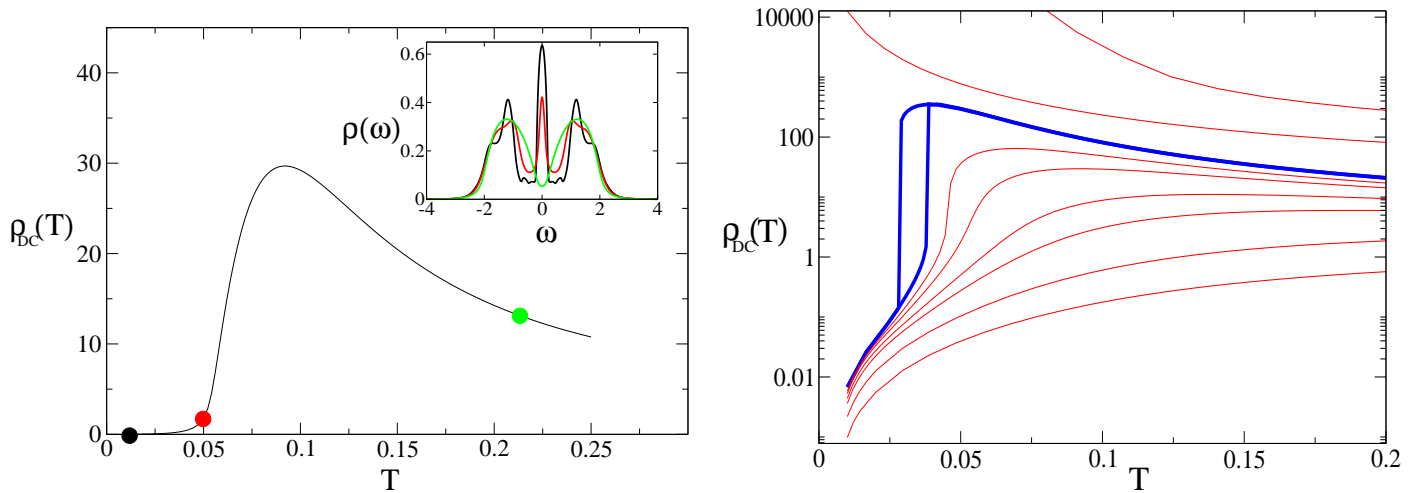


Figure 3: Left: Resistivity in the metallic phase close to the Mott transition ($U = 2.4D$), as a function of temperature, calculated within DMFT using the IPT approximation. For three selected temperatures, corresponding to the three regimes discussed in the text, the corresponding spectral density is displayed in the inset. Right: IPT results for the resistivity for values of U in the metallic regime (lower curves), the coexistence region (bold curve) and the insulating regime (upper two curves).

results displayed in Fig. 3 have been obtained with this technique, and the overall shape of the resistivity curves are qualitatively reasonable. However, the IPT approximation does a poor job on the quasiparticle lifetime in the low-temperature regime. Indeed, we expect on general grounds that, close to the transition, $D \text{Im}\Sigma$ becomes a scaling function [24] of ω/ε_F^* and T/ε_F^* , so that for $T \ll \varepsilon_F^*$ it behaves as: $\text{Im}\Sigma(\omega = 0) \propto D(T/\varepsilon_F^*)^2 \propto T^2/(Z^2D)$ which leads to an enhancement of the T^2 coefficient of the resistivity by $1/Z^2$ as mentioned above. The IPT approximation does not capture this enhancement and yields the incorrect result $\text{Im}\Sigma_{IPT}(\omega = 0) \propto U^2T^2/D^3$. For this reason, we have recently used [23] the numerical renormalization group (NRG) method in order to perform accurate transport calculations within DMFT. This method is very appropriate in this context, since it is highly accurate at low energies and yields real-frequency data[25]. A comparison of the IPT and NRG results for both the resistivity and lifetime is displayed in Fig. 4. The very different curvatures in the low- T regime in fact affects the whole T -dependence of the resistivity. In particular, the resistivity maximum occurs at a temperature much lower than predicted by the IPT approximation. We found this to be important when comparing these calculations to transport data on organics[23]. Both these compounds and Cr-doped V_2O_3 display the various crossovers described above.

4. CRITICAL BEHAVIOUR: A LIQUID-GAS TRANSITION

Progress has been made recently in identifying the critical behaviour at the Mott critical endpoint, both from a theoretical and experimental standpoint.

It has been pointed early on by Castellani *et al.*[26] (see also [27]) that an analogy exists with the liquid-gas transition in a classical fluid. Qualitatively, one can focus on the density of double occupancies (or holes) in each phase: the insulating phase then corresponds to a low-density “gas”, while the metallic phase corresponds to a high-density “liquid”. Recently, this analogy has been given firm theoretical foundations within the framework of a Landau theory [28, 29, 30] derived from DMFT by Kotliar and coworkers. In this framework, a scalar order parameter ϕ is associated with the low-energy electronic degrees of freedom which build up the quasiparticle resonance in the strongly correlated metallic phase close to the transition. This order parameter couples to the singular part of the double occupancy (hence providing a connection to the qualitative picture above), as well as to other observables such as the Drude weight

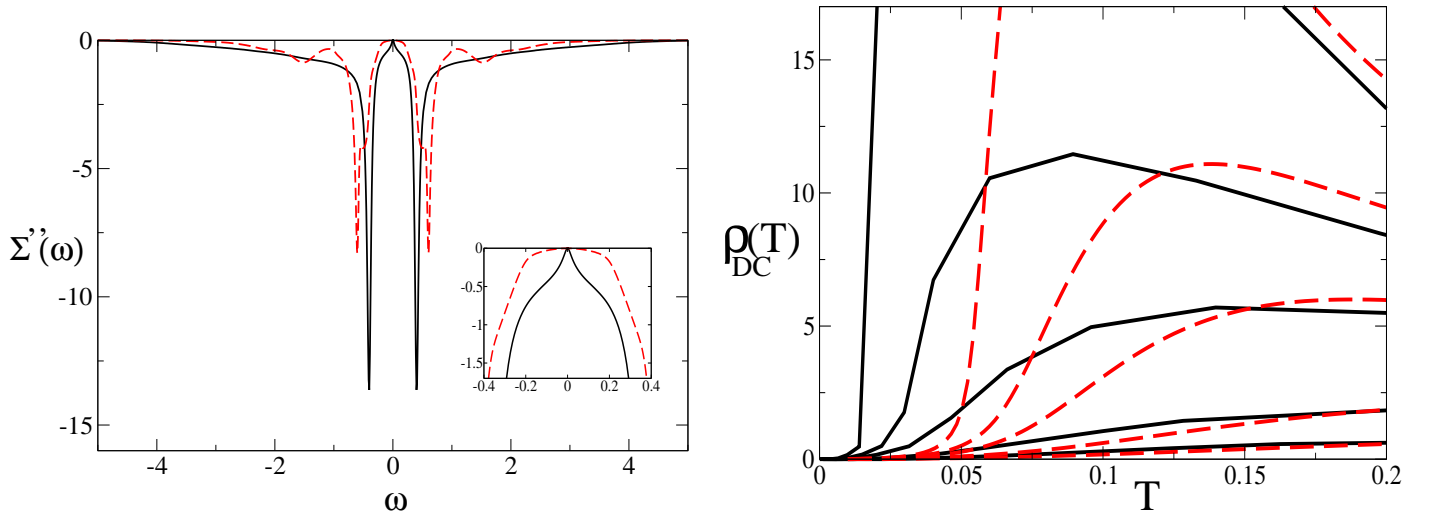


Figure 4: Comparison between the IPT (dashed lines) and NRG methods (plain lines). Left: The low-frequency behaviour of the inverse lifetime $\text{Im}\Sigma'$ clearly displays a critically enhanced curvature, which is not reproduced by IPT. Right: Temperature-dependence of the resistivity in both methods. Note the enhancement of the T^2 term and the lower temperature for the maximum in the NRG results.

or the dc-conductivity. Because of the scalar nature of the order parameter, the transition falls in the Ising universality class. In Table 1, the correspondence between the Ising model quantities, and the physical observables of the liquid-gas transition and of the Mott metal-insulator transition is summarized.

Table 1: Corresponding quantities in the liquid-gas description of the Mott critical endpoint. The associated Landau free-energy density reads $r\phi^2 + u\phi^4 - h\phi$ (a possible ϕ^3 can be eliminated by an appropriate change of variables and a shift of ϕ).

Hubbard model	Mott MIT	Liquid-gas	Ising model
$D - D_c$	$p - p_c$	$p - p_c$	Field h (w/ some admixture of r)
$T - T_c$	$T - T_c$	$T - T_c$	Distance to critical point r (w/ some admixture of h)
Low- ω spectral weight	Low- ω spectral weight	$v_g - v_L$	Order parameter (scalar field ϕ)

In Fig. 5, the dc-conductivity obtained from DMFT in the half-filled Hubbard model (using IPT) is plotted as a function of the half-bandwidth D , for several different temperatures. The curves qualitatively resemble those of the Ising model order parameter as a function of magnetic field (in fact, $D - D_c$ is a linear combination of the field h and of the mass term r in the Ising model field theory). Close to the critical point, scaling implies that the whole data set can be mapped onto a universal form of the equation of state: $\langle\phi\rangle = h^{1/\delta} f_{\pm}(h/|r|^{\gamma\delta/(\delta-1)})$. In this expression, γ and δ are critical exponents associated with the order parameter and susceptibility, respectively: $\langle\phi\rangle \sim h^{1/\delta}$ at $T = T_c$ and $\chi = d\langle\phi\rangle/dh \sim |T - T_c|^{-\gamma}$. f_{\pm} are universal scaling functions associated with $T > T_c$ (resp. $T < T_c$). A quantitative study of the critical behaviour of the double occupancy within DMFT was made in Ref. [29], with the expected mean-field values of the exponents $\gamma = 1, \delta = 3$.

Precise experimental studies of the critical behaviour at the Mott critical endpoint have been performed very recently, using a variable pressure technique, for Cr-doped V_2O_3 [31] and also for the κ -BEDT organic compounds [32]. In the case of V_2O_3 , a full scaling onto the universal equation of state of the liquid-gas

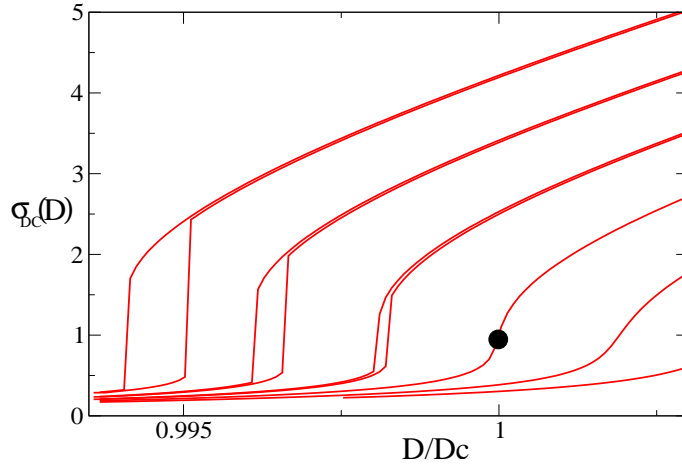


Figure 5: IPT calculation of the dc-conductivity as a function of the half-bandwidth for the half-filled Hubbard model within DMFT, for several different temperatures. Increasing D drives the system more metallic. The curve at $T = T_c$ displays a singularity (vertical slope: dot) and hysteretic behaviour is found for $T < T_c$.

transition could be obtained [31].

5. COUPLING TO THE LATTICE, HOT SPOTS AND MORE...

To conclude, we would like to emphasize some open issues and topics of current interest in connection with the Mott transition and its theoretical description reviewed here.

Lattice degrees of freedom do play a role at the Mott transition in real materials, e.g the lattice spacing changes discontinuously through the first-order transition line in $(V_{1-x}Cr_x)_2O_3$. In the metallic phase, the d-electrons participate in the cohesion of the solid, hence leading to a smaller lattice spacing than in the insulating phase. Both the electronic degrees of freedom and the ionic positions must be retained in order to describe these effects. In Ref. [33] (see also [34], such a model was treated in the simplest approximation where all phonon excitations are neglected. The free energy then reads: $F = K(v - v_0)^2/2 + F_{el}[D(v)]$. In this expression, v is the unit-cell volume, K is an elastic constant and the electronic part of the free-energy F_{el} depends on v through the volume-dependence of the bandwidth. In such a model, the critical endpoint is reached when the electronic response function $\chi = -\partial^2 F_{el}/\partial D^2$ is large enough (but not infinite), and hence the critical temperature T_c of the compressible model is larger than T_c^{el} (at which χ diverges in the Hubbard model). The compressibility $\kappa = (v\partial^2 F/\partial v^2)^{-1}$ diverges at T_c . This implies an anomalous lowering of the sound-velocity at the transition[35], an effect that has been experimentally observed in the κ -BEDT compounds recently [36].

We emphasize that, within DMFT, a purely electronic model can display a first-order Mott transition and a finite-T critical endpoint (associated with a diverging χ), provided that magnetism is frustrated enough so that ordering does not preempt the transition. Whether this also holds for the finite-dimensional Hubbard model beyond DMFT is to a large extent an open question (see [37] for indications supporting this conclusion in the 2D case).

There are also important open questions associated with the role of spatial correlations (inadequately treated by DMFT) in our theoretical understanding of the Mott transition. In the regime where the quasiparticle coherence scale ε_F^* is small as compared to the (effective strength of the) superexchange J , the DMFT picture is certainly deeply modified. A possibility is that near the transition, the Fermi surface divides into “cold” and “hot” regions associated with longer and shorter quasiparticle lifetimes, respectively (as recently found in a cluster DMFT study[38], see also T.Giamarchi *et al.* in these proceedings). Finally, the role of long-wavelength collective modes (in both the charge and spin sectors), and their feedback on quasiparticle properties is also a key issue which requires to go beyond the DMFT framework.

Acknowledgements

We are most grateful to the experimental group at Orsay (D. Jerome, P. Limelette, C. Pasquier, P. Wzietek) as well as to P. Batail, P. Metcalf, C. Meziere and J.M. Honig, for a wonderful collaboration. We also thank J.Allen, S.R. Hassan, M. Imada, G. Kotliar, H.R. Krishnamurthy, and M. Rozenberg for numerous discussions.

References

- [1] M. Imada, A. Fujimori, and Y. Tokura, *Rev. Mod. Phys.* **70**, 1039 (1998).
- [2] W. Bao, C. Broholm, G. Aeppli, P. Dai, J. M. Honig, and P. Metcalf, *Phys. Rev. Lett.* **78**, 507 (1997).
- [3] G. Kotliar, *Physica B* **259-261**, 711 (1999).
- [4] G. Misguich and C. Lhuillier, *Two-dimensional quantum antiferromagnets* (World Scientific, Singapore, 2003), cond-mat/0310405.
- [5] Y. Shimizu, K. Miyagawa, K. Kanoda, M. Maesato, and G. Saito, cond-mat/0307483.
- [6] M. Imada, T. Mizusaki, and S. Watanabe, cond-mat/0307022 .
- [7] D. B. McWhan, A. Menth, J. P. Remeika, W. F. Brinckman, and T. M. Rice, *Phys. Rev. B* **7**, 1920 (1973).
- [8] S. Lefebvre, P. Wzietek, S. Brown, C. Bourbonnais, D. Jérôme, C. Mèzière, M. Fourmigué, and P. Batail, *Phys. Rev. Lett.* **85**, 5420 (2000).
- [9] A. Georges, G. Kotliar, M. Rozenberg, and W. Krauth, *Rev. Mod. Phys.* **68**, 13 (1996).
- [10] M. J. Rozenberg, X. Y. Zhang, and G. Kotliar, *Phys. Rev. Lett.* **69**, 1236 (1992); A. Georges and W. Krauth, *Phys. Rev. Lett.* **69**, 1240 (1992); X. Y. Zhang, M. J. Rozenberg, and G. Kotliar, *Phys. Rev. Lett.* **70**, 1666 (1993); A. Georges and W. Krauth, *Phys. Rev. B* **48**, 7167 (1993); M. J. Rozenberg, G. Kotliar, and X. Y. Zhang, *Phys. Rev. B* **49**, 10181 (1994); L. Laloux, A. Georges, and W. Krauth, *Phys. Rev. B* **50**, 3092 (1994)
- [11] A. Georges and G. Kotliar, *Phys. Rev. B* **45**, 6479 (1992).
- [12] M. Jarrell, *Phys. Rev. Lett.* **69**, 168 (1992).
- [13] A. Fujimori, I. Hase, H. Namatame, Y. Fujishima, Y. Tokura, H. Eisaki, S. Uchida, K. Takegahara, and F. M. F. de Groot, *Phys. Rev. Lett.* **69**, 1796 (1992).
- [14] S. K. Mo, J. D. Denlinger, H. D. Kim, J. H. Park, J. W. Allen, A. Sekiyama, A. Yamasaki, K. Kadono, S. Suga, Y. Saitoh, T. Muro, P. Metcalf, G. Keller, K. Held, V. Eyert, V. I. Anisimov, and D. Vollhardt, *Phys. Rev. Lett.* **90**, 186403 (2003).
- [15] A. Y. Matsuura, H. Watanabe, C. Kim, S. Doniach, Z. X. Shen, T. Thio, and J. W. Bennett, *Phys. Rev. B* **58**, 3690 (1998).
- [16] K. Maiti, D. D. Sarma, M. Rozenberg, I. Inoue, H. Makino, O. Goto, M. Pedio, and R. Cimino, *Europhys. Lett.* **55**, 246 (2001).
- [17] A. Sekiyama, H. Fujiwara, S. Imada, H. Eisaki, S. I. Uchida, K. Takegahara, H. Harima, Y. Saitoh, and S. Suga, preprint cond-mat/0206471.

- [18] M. J. Rozenberg, G. Kotliar, H. Kajueter, G. A. Thomas, D. H. Rapkine, J. M. Honig, and P. Metcalf, *Phys. Rev. Lett.* **75**, 105 (1995).
- [19] J. Eldridge, K. Kornelsen, H. Wang, J. Williams, A. Crouch, and D. Watkins, *Sol. State. Comm.* **79**, 583 (1991).
- [20] L. Liu, J. Allen, O. Gunnarsson, N. Christansen, and O. Andersen, *Phys. Rev. B* **45**, 8934 (1992).
- [21] P. Majumdar and H. Krishnamurthy, *Phys. Rev. B* **52**, (1995).
- [22] J. Merino and R. H. McKenzie, *Phys. Rev. B* **61**, 7996 (2000).
- [23] P. Limelette, P. Wzietek, S. Florens, A. Georges, T. A. Costi, C. Pasquier, D. Jerome, C. Meziere, and P. Batail, *Phys. Rev. Lett.* **91**, 016401 (2003).
- [24] G. Moeller, Q. Si, G. Kotliar, M. Rozenberg, and D. S. Fisher, *Phys. Rev. Lett.* **74**, 2082 (1995).
- [25] R. Bulla, T. A. Costi, and D. Vollhardt, *Phys. Rev. B* **64**, 45103 (2001).
- [26] C. Castellani, C. DiCastro, D. Feinberg, and J. Ranninger, *Phys. Rev. Lett.* **43**, 1957 (1979).
- [27] A. Jayaraman, D. B. McWhan, J. P. Remeika, and P. D. Dernier, *Phys. Rev. B* **2**, 3751 (1970).
- [28] G. Kotliar, *Eur. J. Phys. B* **27**, 11 (1999).
- [29] G. Kotliar, E. Lange, and M. J. Rozenberg, *Phys. Rev. Lett.* **84**, 5180 (2000).
- [30] M. J. Rozenberg, R. Chitra, and G. Kotliar, *Phys. Rev. Lett.* **83**, 3498 (1999).
- [31] P. Limelette, A. Georges, D. Jérôme, P. Wzietek, P. Metcalf, and J. Honig, *Science* **302**, 89 (2003).
- [32] F. Kagawa, T. Itou, K. Miyagawa, and K. Kanoda, preprint cond-mat/0307304.
- [33] P. Majumdar and H. Krishnamurthy, *Phys. Rev. Lett.* **73**, (1994).
- [34] M. Cyrot and P. Lacour-Gayet, *Sol. State Comm.* **11**, 1767 (1972).
- [35] J. Merino and R. McKenzie, cond-mat/0007173.
- [36] D. Fournier, M. Poirier, M. Castonguay, and K. Truong, *Phys. Rev. Lett.* **90**, 127002 (2003).
- [37] S. Onoda and M. Imada, cond-mat/0304580.
- [38] O. Parcollet, G. Biroli, and G. Kotliar, cond-mat/0308577.